AACR 2026, POSTER # 4747

Integrated tumor histoculture and same-cell spatial multiomics link biosignatures to immune checkpoint blockade responses in head and neck cancer

Yi Cui[2], Moumita Nath[1], Isabel Lee[2], Dan McGuire[2], Michael Patrick[2], Jobin K Paul[1], Kowshik Jaganathan[1], Biswajit Das[1], Pradeepa S Sundaram[1], Poojitha Nagapushnam[1], Mohit Malhotra[1], Shanshan He[2], Joseph Beechem[2], Satish Sankaran[1]

[1]Farcast Biodynamics [2]Bruker Spatial Biology

Introduction

Response to immune checkpoint blockade (ICB) in head and neck squamous cell carcinoma (HNSCC) depends on more than immune infiltration alone; it also requires productive spatial organization and cross-talk among immune, stromal, and tumor compartments. The TruTumor™ histoculture platform preserves the native architecture of patient-derived tumors and enables functional testing of immunotherapy response in an FDA NAM-aligned setting. Previous TruTumor studies linked anti-PD-1 response to CTL infiltration into tumor nests and suggested that addition of anti-CTLA-4 can rescue tumors with incomplete response. To better define the spatial mechanisms underlying these effects, we combined TruTumor with CosMx® SMI same-cell spatial multiomics in HNSCC explants treated with nivolumab or nivolumab + ipilimumab. Our current analyses show that the strongest response-associated features are immune-tumor spatial access and tumor-boundary immune coordination, rather than immune abundance alone. Responding samples are characterized by greater immune access to tumor cells and more organized boundary niches containing effector CD8 T cells, antigen-presenting myeloid cells, and B/plasma cell-associated support states, whereas fibroblast barriers, myeloid suppressive programs, and tumor-state composition appear to contribute to a more patient-specific manner. These results support a model in which combination ICB improves efficacy by restructuring the tumor-immune interface into a more productive, coordinated immune niche.

Patient tumor histoculture for subcellular transcriptome-wide multiomic profiling

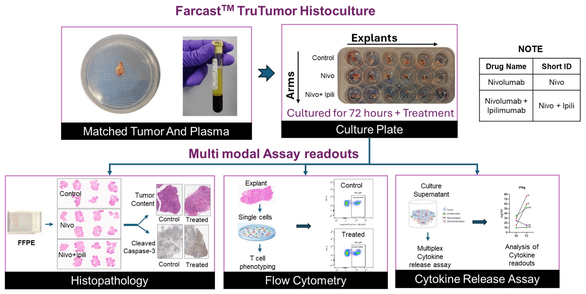

Fig 1. Schematic representation of Farcast™ TruTumor histoculture platform work-flow and downstream assays used for treatment response evaluation.

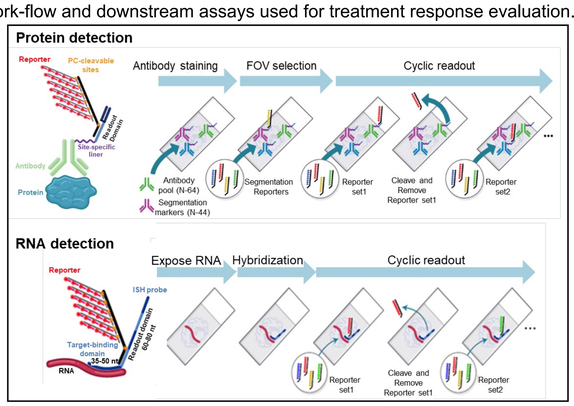

Fig 2. The CosMx SMI multiomics assay sequentially detects protein and RNA targets with oligonucleotide-conjugated antibodies and barcoded RNA probes via sequential rounds of reporter binding and fluorescence imaging.

TruTumor platform enables personalized classification of response to treatment

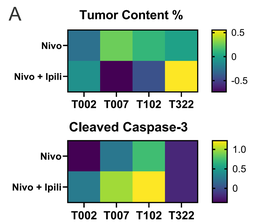

Sample ID	Nivo	Nivo + Ipili
T002	R	NR
T007	NR	R
T102	MR	R
T322	NR	NR

Combination therapy does not always guarantee better response than monotherapy

Fig 3. Response evaluated using tumor cytotoxicity parameters. (A) Heatmaps of $\log_2$(fold change) of treated relative to control arms showing tumor content (top panel) and Cleaved Caspase-3 expression within tumor (bottom panel). (B) Response classification for Nivolumab and Nivolumab + Ipilimumab treatment.
R = Responder; MR = Moderate Responder; NR = Non-Responder.

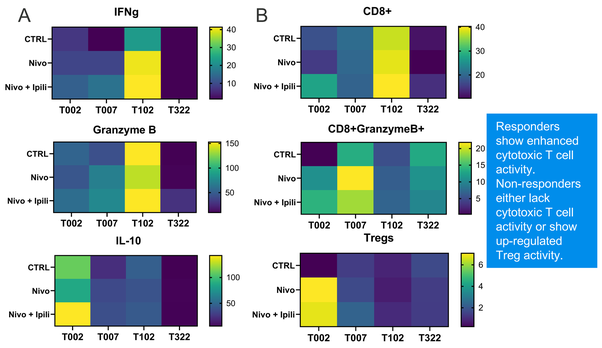

Fig 4. Heatmap analysis of key immunological parameters across control and treated arms. (A) Cytokine release IFNg (top), Granzyme B (middle) and IL-10 (bottom), and (B) Flow cytometry based immune phenotyping; CD8+ (top), CD8+GranzymeB+ (middle) and Tregs (bottom).

CosMx multiomic profiling provides complete molecular information for each explant

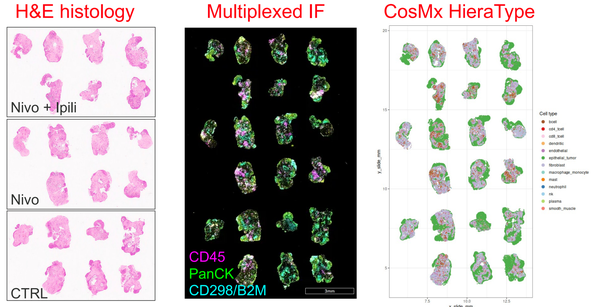

Fig 5. A multi-modal spatial dataset was obtained for each tumor sample, enabling comprehensive tissue exploration with subcellular resolution.

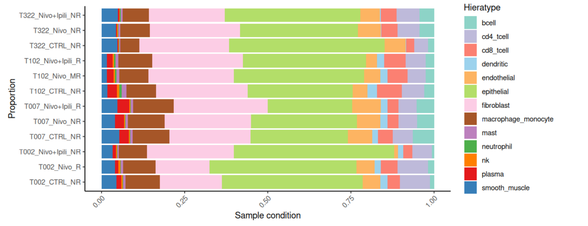

Fig 6. The CosMx multiomic assay supported robust cell type annotation, which revealed distinct tissue compositions in differently treated TruTumor samples.

Immune cell accessibility to tumor cell is the key factor to predict ICB therapy responses

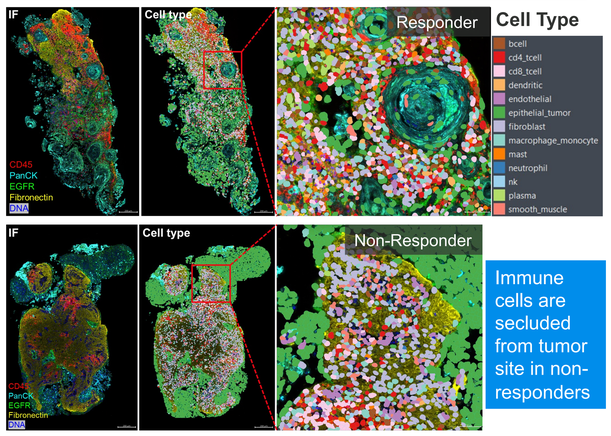

Fig 7. Spatial multiomic exploration showed significant difference in tumor-immune proximity and local mixing diversity.

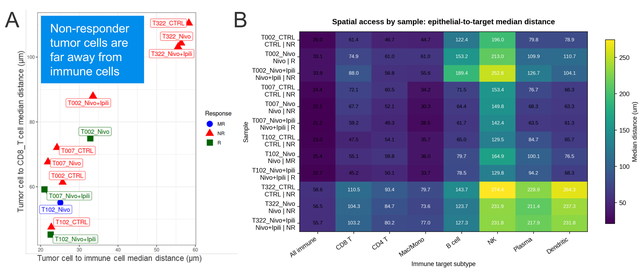

Fig 8. (A) Overview of tumor-immune distance per treatment condition. (B) Heatmap of median distance from each tumor cell to the nearest immune cell type per treatment condition.

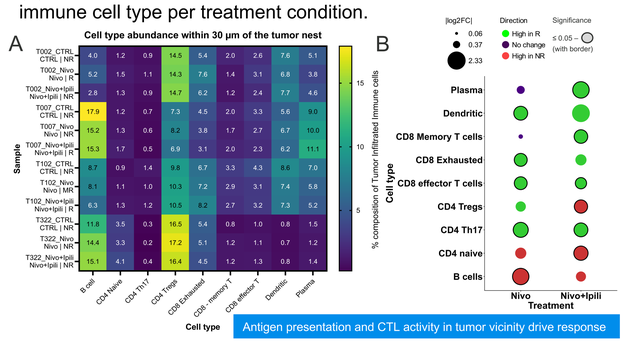

Fig 9. (A) Cell type abundance within 30 µm of the tumor nest. (B) Significant Tumor infiltrated immune cells composition across samples.

Fibroblast barrier blocks immune access to tumor in non-responders

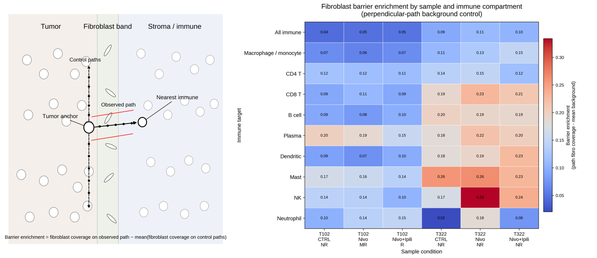

Fig 10. Fibroblast barrier was quantified with the occurrence frequency of fibroblasts (path coverage) from a tumor cell to its nearest immune cell neighbor.

Tissue microenvironment shapes regional immune functions and can be shifted by ICB

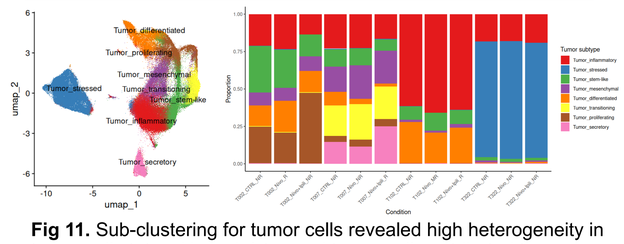

Fig 11. Sub-clustering for tumor cells revealed high heterogeneity in tumor cell status. Hypoxic/stressed tumor cell contributed to a non-responding outcome, while inflammatory tumor cell favored the ICB treatment.

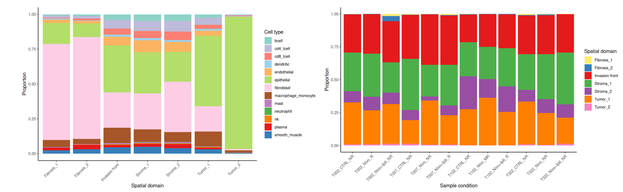

Fig 12. Novae domains categorized the tissues to transcriptomically distinct neighborhoods, with each tumor sample harboring a unique composition of domains.

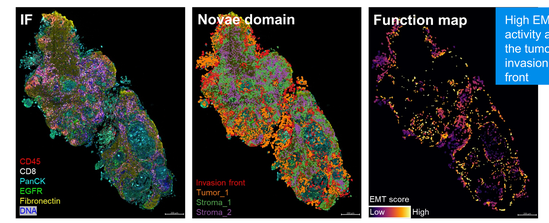

Fig 13. Identified Novae domains can be connected to other layers of molecular information, such as protein expression patterns and EMT activity.

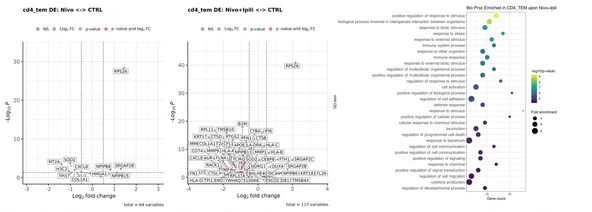

Fig 14. Domain specific DE and GO analyses uncovered that CD4 effector memory T cells were pre-conditioned by Nivo+Ipili to a more active state in stromal region (Stroma_1) close to the invasion front in responders.

Conclusions

- TruTumor explant culture system and CosMx same-cell multiomics enables functional, spatially resolved ICB response profiling with subcellular resolution and whole-transcriptome coverage.
- Tumor-immune proximity and accessibility is the primary driving factor to predict ICB responses in HNSCC patients.
- Fibroblast barriers physically block immune access in a subset of non-responders, suggesting potential synergistic effect between ICB and anti-fibrosis agents.
- Tissue microenvironment domain-specific analyses uncover response mechanisms beyond bulk or cell-type abundance.

REFERENCES
1. Basak NP, *et al.,* Nat Comm 2024. https://doi.org/10.1038/s41467-024-45723-z
2. Khafizov R, *et al.,* BioRxiv 2024. https://doi.org/10.1101/2024.11.27.625536
3. Williams C, *et al.,* BioRxiv 2025. https://doi.org/10.64898/2025.12.19.695622